2021

POLYA: A TOOL FOR ADJUDICATING COMPETING ANNOTATIONS OF BIOLOGICAL SEQUENCES

Kaitlin Carey

POLYA: A TOOL FOR ADJUDICATING COMPETING ANNOTATIONS OF BIOLOGICAL SEQUENCES

By

Kaitlin Carey

Bachelor of Science, The University of Montana, Missoula, MT, 2014

Thesis

presented in partial fulfillment of the requirements
for the degree of

Master of Science
in Computer Science

The University of Montana
Missoula, MT

Autumn 2020

Approved by:

Ashby Kinch Ph.D., Dean
Graduate School

Travis Wheeler Ph.D., Chair
Computer Science

Jesse Johnson Ph.D.
Computer Science

Robert Hubley, Senior Software Engineer
Institute for Systems Biology, Seattle, WA

Carey, Kaitlin, M.S., January 2021 Computer Science

PolyA: a tool for adjudicating competing annotations of biological sequences

Chairperson: Travis Wheeler

Annotation of a biological sequence is usually performed by aligning that sequence to a database of known sequence elements. When that database contains elements that are highly similar to each other, the proper annotation may be ambiguous, because several entries in the database produce high-scoring alignments. Typical annotation methods work by assigning a label based on the candidate annotation with the highest alignment score; this can overstate annotation certainty, mislabel boundaries, and fails to identify large scale rearrangements or insertions within the annotated sequence. Here, I present a new software tool, PolyA, that adjudicates between competing alignment-based annotations by computing estimates of annotation confidence, identifying a trace with maximal confidence, and recursively splicing/stitching inserted elements. PolyA communicates annotation certainty, identifies large scale rearrangements, and detects boundaries between neighboring elements.

ACKNOWLEDGMENTS

I'd like to thank my advisor, Travis Wheeler, for endless support, accessibility, problem solving, algorithm design, mathematical formula derivation, revising/editing my writing, and questions answered at all hours of the day; without him none of this would be possible. I'd also like to thank John McCutcheon who introduced me to computer science and enabled me to discover this passion. I'd like to thank George Lesica for mentoring me in better software practices, Jack Roddy for using his software SODA to create visualizations, Audrey Shingleton for her addition of the tandem repeat analysis, Daniel Olson for using his software ULTRA as a tandem repeat detector and Robert Hubley, Arian Smit and Jeb Rosen (and Jeb came up with the AAAAAAAAAAAAAAAA:PolyA name) for establishing motivation for the software and supplying mechanisms for validation. I'd also like to thank all members of the Wheeler lab for ideas, emotional support, and fun times at conferences. And finally, I'd like to thank my friends and family for supporting me and enduring endless practice talks and presentations. I am very grateful for NIH grants P20GM103546 and 5U24HG010136 for funding my research.

TABLE OF CONTENTS

LIST OF FIGURES

LIST OF TABLES

CHAPTER 1 INTRODUCTION

Biological Sequences

A genome is the set of genetic material in an organism, and it contains complete instructions for how the organism will grow and function. The genome of an organism is stored in long strings of DNA made of linearly-connected components called nucleotides. DNA contains 4 nucleotides, each of which is represented as a letter: A, C, T and G. The human genome, for example, is about 3 billion nucleotides in length, while the smallest viral genomes can be as short as a thousand nucleotides. Related organisms have more similar DNA sequences, while less related organisms have further diverged sequences. Understanding the genetic makeup of an organism provides insight into health, medicine, agriculture, and more, while also allowing us to understand evolutionary history and processes. Annotating recognizable features in the genome is an import step in this pursuit.

Genome Annotation

Genome annotation is the process of assigning labels to a sequence of nucleotides, and is typically based on comparison of such sequences to a database of known sequence elements called query sequences. This comparison is called sequence alignment, which amount to finding good ways to line up the sequence of the genome to one or more of the sequences in the database. A score is assigned to an alignment that corresponds to how well the strings match. If these database sequences match reasonably well to a section of the genome, we assign the corresponding label to that genomic region (see Figure 1.1). If the genomic sequence has good-scoring alignments to multiple database sequences, current annotation methods typically adjudicate the target as belonging to the element with the highest alignment score. This winner-takes-all approach is insufficient for some use cases.

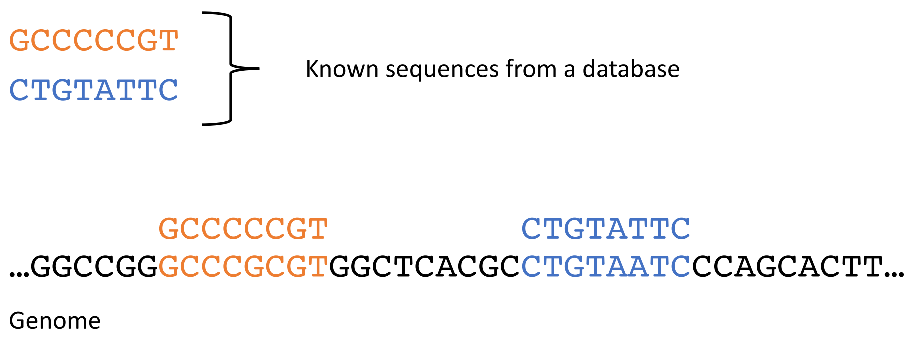
GCCCCCGT
CTGTATTC
Known sequences from a database
GCCCCCGT
CTGTATTC
…GGCCGGGCCCGCGTGGCTCACGCCTGTAATCCCAGCACTT…
Genome

Figure 1.1: Biological sequence annotation is performed by comparing a collection of known sequences from a database, to your genomic or target sequence. Here, the blue and orange sequences from the database match reasonably well to genomic locations. Then, the corresponding locations are given the labels 'blue' and 'orange'.

Biological events that complicate annotation

Competing annotations

When the database of known sequences contains elements that are similar to each other, many related elements may align with a high score to the same region of the target sequence being annotated, sometimes overlapping in non-trivial ways. From these competing annotations software must 'decide' which is the true annotation at that location; we call this process *adjudication* (see Figure 1.2). The winner-takes-all approach of sequence annotation overstates annotation certainty. The existence of multiple related elements is common, even in databases designed to accumulate sequence instances into families. For example, in the Dfam [1] database of transposable element families, some abundant families are divided into highly similar subfamilies in order to represent family history or improve annotation sensitivity. Similarly, the Pfam [2] database of protein domains groups similar families into 'clans', as does the Rfam [3] database of non-coding RNA families; in both cases, clan competition selects the longest and highest scoring hit when multiple clan members match the annotated sequence.

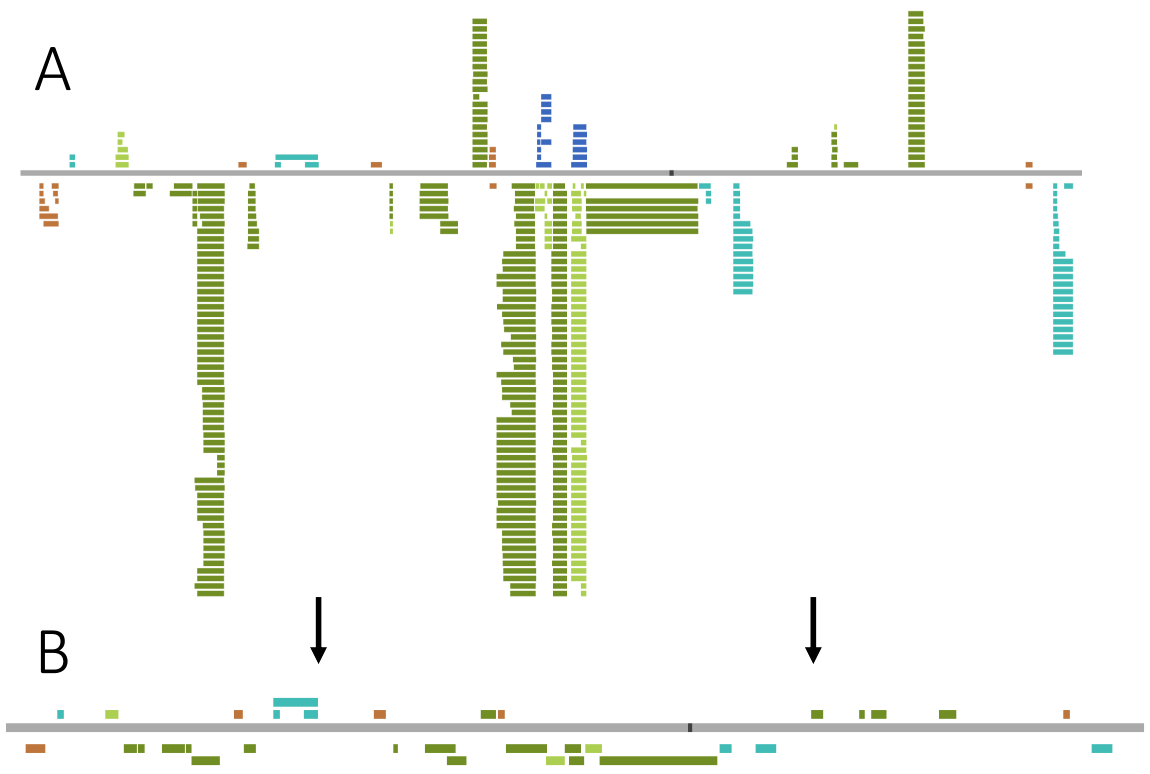

Figure 1.2: A. Several competing query sequences (blue, green and orange rectangles) from a database match to the same genomic regions (grey rectangle). B. The annotation process produces chooses the best match from the competitors and labels the genomic region. [1]

Adjacent neighbors

Due to the nature of sequence alignment, often times the alignment is extended past the boundary of relatedness. This can result in boundaries between adjacent elements being unclear (see Figure 1.3).

Recombination

Homologous recombination (usually) occurs as the result of a double-stranded break in a strand of DNA; during the repair process a similar sequence is used as a template for repair, and in some cases may itself break and ligate to the first. The resulting sequence is chimeric - part one element and part the other element. During the alignment process, full length instances of both database

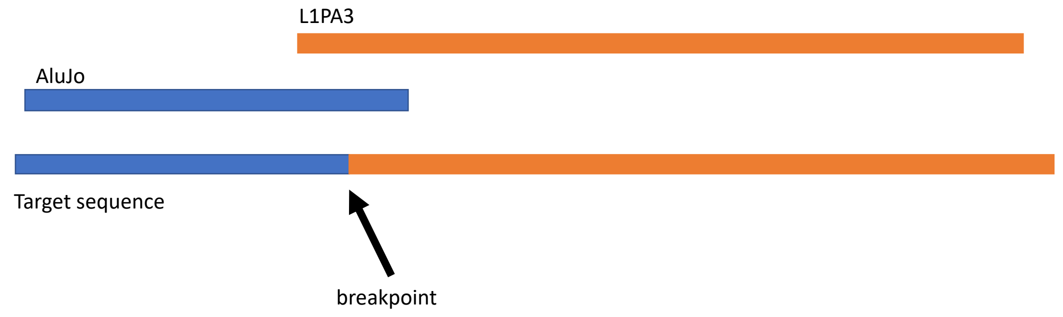

Figure 1.3: The terminal end of AluJo alignment overlaps with the start of the L1PA3 alignment. This is caused by over extension in one or both alignments. The actual boundary between these adjacent elements is unknown.

sequences may align to the recombined region (one better matching the first part, the other better-matching the second part), obscuring the recombination (see Figure 1.4). Current annotation methods provide no basis for recognizing rearrangements such as in homologous recombination.

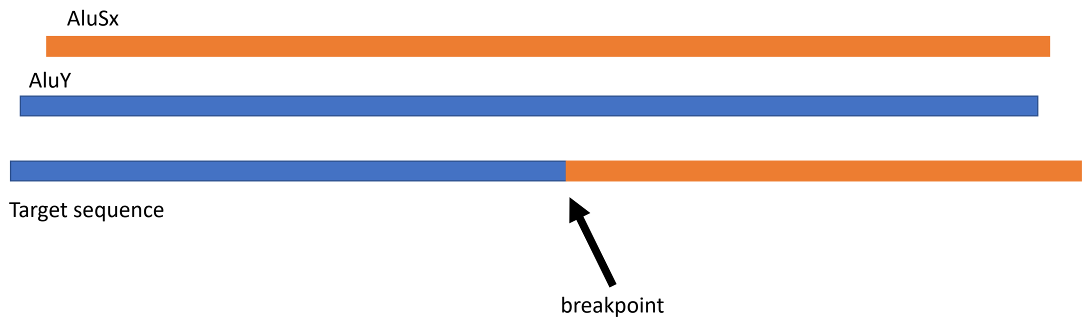

Figure 1.4: In the target sequence, half the blue sequence (AluY) has been recombined with half of the orange sequence (AluSx). Full length instances of AluY and AluSx have aligned to this region. The annotation process will choose the single best match completely missing the recombination.

Nesting

Certain genomic activity (specifically: the replication of transposable elements, see below) can result in sequences that have created copies of themselves and placed those copies elsewhere in the genome. Sometimes the copy is inserted inside of another element (see Figure 1.5). Current annotation methods can recognize all of the resulting segments, but can not directly identify fragments from the sub-divided sequence - expert systems such as the ProcessRepeats post-processing script in RepeatMasker [4] perform such fragment stitching based on extensive domain-specific knowledge.

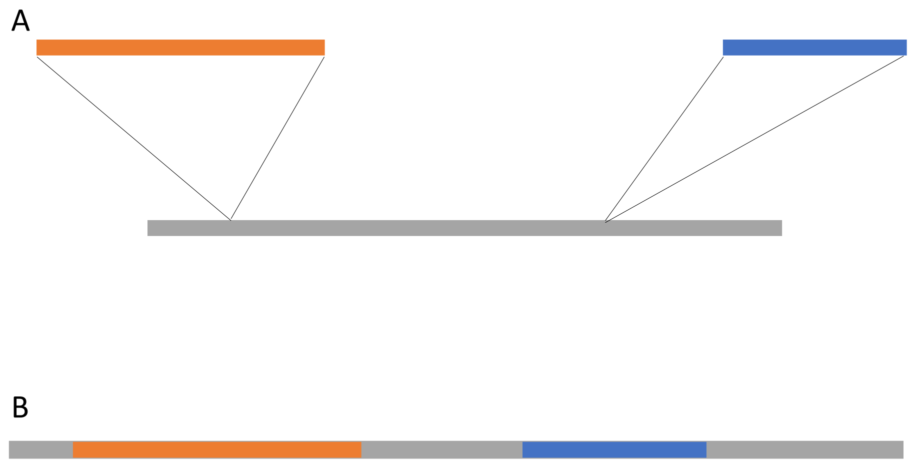

Figure 1.5: A. The blue and orange sequences have inserted themselves inside of the gray sequence. B. This results in separated segments from the original gray sequence.

Transposable elements (TE)

TEs are sequences of DNA that move or replicate from one region of the genome to another, often via a copy/paste mechanism. When a TE has distributed numerous copies of itself across a genome, the resulting copies are said to belong to the same family. If those copies came in bursts, with evolutionary pressures influencing the success of a copy, the results of each burst may be thought of as a subfamily. These subfamily sequences can be very similar to each other [1].

Our analysis focuses on transposable elements, because they present all of the annotation challenges listed above. High levels of sequence similarity between subfamilies can cause several database sequences to align well to a specific genomic sequence, necessitating adjudication between competing annotations. In addition, integration of one element into another is a hallmark of TE activity, so that split sequences and unclear boundaries are very common. Furthermore, due to sequence similarity between elements, rearrangements are common in TEs.

Current TE annotation

To our knowledge, RepeatMasker (specifically its ProcessRepeats function) represents the most complex TE adjudication engine in use today, with expert knowledge built into the software to select between overlapping competing annotations, and even control the order of candidate alignments (when known) in order to recursively splice out inserted elements. In addition, RepeatMasker identifies cases in which multiple candidate annotations have nearly-identical scores, and reduces annotation specificity in some cases of ambiguity (e.g. labeling a sequence simply 'Alu' when several competing Alu subfamilies all share near-identical scores). My goal in developing the software described here has been to replace this domain-specific framework with one that works with generic alignment tools, requiring no expert knowledge of the underlying family structure, and improving representations of confidence, overlap, recombination, and insertions/stitching.

PolyA

I have devised a simple method for computing confidence in (sub)family membership in the face of competing sequence alignments, making it possible to report confidence values for sequence labels, rather than simply reporting a single 'winner' from all possible matches. I then extended this confidence scoring method to compute residue-specific annotation based on the ensemble of competing alignments, assigning labels (with annotation confidence) to each residue of the target sequence.

In the following sections, I introduce PolyA, short for 'AAAAAAAAAAAAAAA: Automatically Adjudicate Any And All Arbitrary Annotations, Astutely Adjoin Abutting Alignments, And Also Amputate Anything Amiss'. I demonstrate that it (i) reports a meaningful measure of annotation certainty, (ii) recognizes many instances of homologous recombination, (iii) effectively stitches sequence element segments resulting from nested insertions, (iv) accurately locates boundaries between overlapping candidate annotations, and (v) yields adjudicated annotation results that agree with those of RepeatMasker without resorting to complex and domain-specific expert system logic. I follow with a complete description of the methods supporting the observed results.

To my knowledge, PolyA is the first tool that computes a measure of annotation confidence in the face of competing alignments, and the first to establish a principled framework for selecting the boundary cutoffs between overlapping annotations. PolyA is available for download at https://github.com/TravisWheelerLab/polyA.

The work described here is largely my own, but significantly benefited from infusions of effort by several members of the Wheeler lab (see Acknowledgements for details). Because the final results depend on these contributions, the remainder of this document will describe effort in the first-person-plural ("we") rather than singular ("I").

CHAPTER 2 METHODS

Computing confidence in annotation of a full sequence

We can compute a measure of confidence that an annotated sequence belongs to a subfamily i by leveraging the probabilistic underpinnings of alignment scores. We have described these calculations in [5], but reproduce them here for completeness.

Given $Q = q_1, q_2, ..., q_n$ competing subfamily annotations of genomic sequence t, we define $P(q_i|t)$ as the probability that the true label of t is q_i, and the confidence that q_i is the correct label is

$$\text{Conf}(q_i|t) = \frac{P(q_i|t)}{\sum_j P(q_j|t)} \tag{2.1}$$

Assuming a uniform distribution over Q, $P(q_i|t) \propto P(t|q_i)$, so that

$$\text{Conf}(q_i|t) = \frac{P(t|q_i)}{\sum_j P(t|q_j)} \tag{2.2}$$

In scoring matrices used for sequence alignments, the score for aligning a pair of letters is a log odds ratio [6], typically scaled by factor λ then rounded to the nearest integer value. Under the simplifying assumption that gap costs map to probabilities [7], the overall alignment score corresponds to a scaled log of the ratio of the probability of observing t if it is homologous to q_i vs the probability of observing t under a random (non-homology) model:

$$\text{score}(t, q_i) = \lambda \cdot \lg \frac{P(t|q_i)}{P(t|R)} \tag{2.3}$$

After straightforward algebraic manipulation

$$P(t|q_i) = P(t|R) \cdot 2^{score(t,q_i)/\lambda} \tag{2.4}$$

and following substitution into equation 2.2

$$\text{Conf}(q_i|t) = \frac{2^{score(t,q_i)/\lambda}}{\sum_j 2^{score(t,q_j)/\lambda}} \tag{2.5}$$

This derivation depends on the assumption that all competing family annotations are equally likely; in the case of non-uniform priors, with $P(q_k)$ defined as the prior probability of annotation q_k, the computation may be adjusted as:

$$\text{Conf}(q_i|t) = \frac{2^{score(t,q_i)/\lambda} \cdot P(q_i)}{\sum_j P(q_j) \cdot 2^{score(t,q_j)/\lambda}} \tag{2.6}$$

Residue-specific confidence, tracing through competing annotations

A natural mechanism for sub-family annotation would be to develop a jumping profile hidden Markov model (jpHMM) [8], representing the full contingent of candidate families, then to align genomic sequence to such a jpHMM. Posterior probabilities calculated on a nucleotide-resolution basis could work in lieu of the above calculations, and could also identify recombinations and boundary transitions between adjacent overlapping alignments. Unfortunately, such a model would be prohibitively computationally expensive. Here, we describe an efficient method for computing annotation confidence at residue-level resolution, followed by a dynamic programming algorithm that traces a maximum confidence labeling of the annotated genome sequence.

To compute residue-specific estimates of annotation confidence, we first modify the above full-sequence confidence calculations to compute confidence across length-w windows. For each position j in the annotated sequence of length L, we consider a window centered on j (trimmed at the ends) as follows: let $s = \max(1,\ j - \lfloor w/2 \rfloor)$ and $e = \min(L,\ j + \lfloor w/2 \rfloor)$, and compute the windowed confidence $Conf_{i,j}$ as above, considering only the scores of sub-alignments that cover sequence positions in the window $s..e$. By computing confidence within windows, our tool can account for the fact that one region of sequence is better explained by one candidate annotation, while another region is best explained by an alternate annotation.

The choice of window length is arbitrary - it should be long enough to smooth out the influence of individual mutations, but short enough to capture annotation transition points; PolyA sets the window length to $w = 31$ by default. In order to produce a less-granular picture of annotation confidence, PolyA computes residue-specific estimates for each position j by capturing an unweighted average of the confidence calculations of all windows that include position j. Individual mutations (especially gaps) can cause a single window's score to vary substantially; this effect is muted by capturing confidence on a windowed basis.

$$\text{Conf\_avg}_{i,j} = \frac{\sum_{k=s}^{e} \text{Conf}_{i,k}}{w} \tag{2.7}$$

Based on these per-residue confidence values, PolyA computes a maximum confidence trace through candidate annotations across the length of the annotated sequence, using the dynamic programming (DP) recurrence shown in Figure 2.1, in which each row is a candidate annotation i, and each column is a sequence position j.

Two additional candidate annotations are considered, beyond those provided in the form of sequence alignments. (1) Candidate short tandem repeats (STRs) are identified using the tool ULTRA [9], which provides per-residue log-odds ratio scores that fit naturally into the PolyA confidence calculations; these are simply treated as an additional candidate annotation. (2) In some cases, a single low-quality annotation may extend slightly beyond a clearly-preferred annotation; if PolyA is forced to choose among available annotations, a small clip of this low-quality annotation will be selected. PolyA avoids this outcome by including what we call a *skip state*; when the annotation trace is in a skip state, the corresponding sequence is assigned no annotation. Skip states are given a special default score (such that they will out-compete low-quality candidate annotations).

To encourage annotation continuity, transitioning from one annotation candidate to a different annotation is heavily penalized. The penalty for transitioning to/from the skip state is reduced.

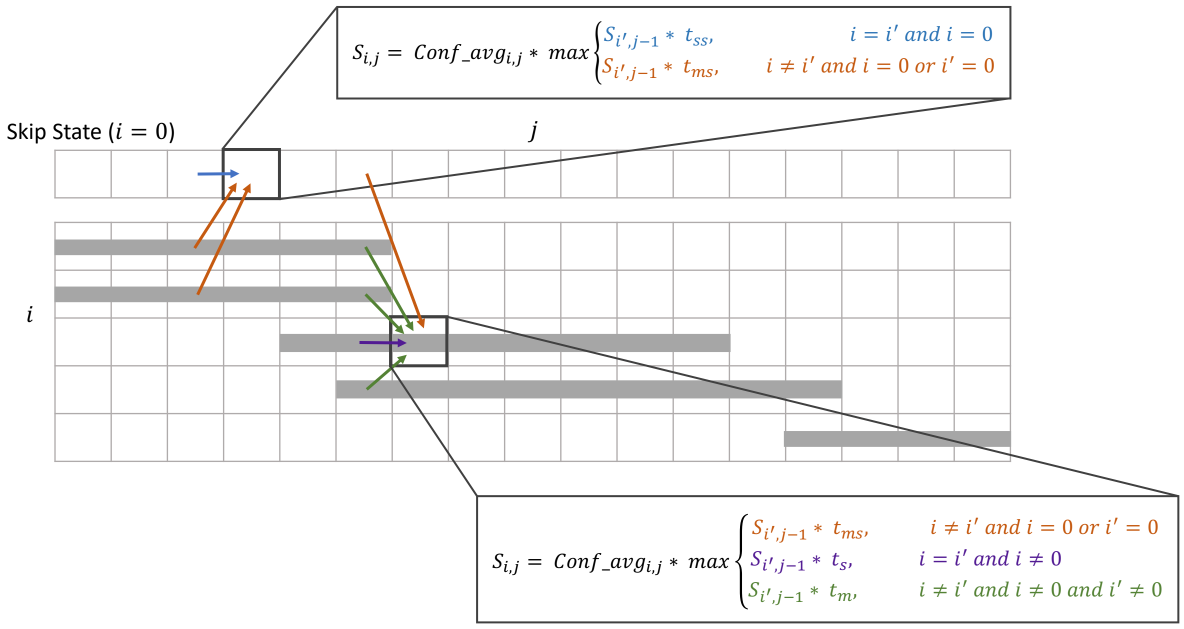

$S_{i,j} = Conf\_avg_{i,j} * max \begin{cases} S_{i',j-1} * t_{ss}, & i = i' \text{ and } i = 0 \\ S_{i',j-1} * t_{ms}, & i \neq i' \text{ and } i = 0 \text{ or } i' = 0 \end{cases}$
Skip State ($i = 0$)
j
i
$S_{i,j} = Conf\_avg_{i,j} * max \begin{cases} S_{i',j-1} * t_{ms}, & i \neq i' \text{ and } i = 0 \text{ or } i' = 0 \\ S_{i',j-1} * t_{s}, & i = i' \text{ and } i \neq 0 \\ S_{i',j-1} * t_{m}, & i \neq i' \text{ and } i \neq 0 \text{ and } i' \neq 0 \end{cases}$

Figure 2.1: In the implicit dynamic-programming matrix, each column represents a position in the genome, and each row represents a candidate annotation family. In this figure, a gray bar corresponds to an alignment of the sequence for family i over a range of genome positions. Cells covered by a gray bar represent positions covered by an alignment - confidence ($Conf\_avg_{i,j}$) and score ($S_{i,j}$) values are computed only these positions; other cells have an implicit value of zero. Because this describes a very sparse matrix, values are stored as a sparse set of (i,j,conf_avg) tuples. Transition probabilities are: t_s ('stay in the same row'), t_m ('move to a new non-skip-state row'), t_{ms} ('move between the skip-state row and a non-skip-state row'), and t_{ss} ('stay in the skip-state row'). Default values are: $t_m = 1e-55$, $t_{ms} = \sqrt{t_m}$, $t_s = 1 - t_m - t_{ms}$, $t_{ss} = 1 - t_{ms}$.

Because an annotated sequence may exceed the length of any single candidate annotation, the Conf_avg$_{i,j}$ matrix is sparse; the DP implementation performs correspondingly sparse calculations to avoid excessive time and space resource use.

A maximal trace through the sparse DP matrix described in Figure 2.1 yields an ordered series of labeled regions over the target sequence. These regions may identify transitions between adjacent elements and recombination or insertion events.

Recursive splicing of insertions, and stitching of surrounding sequences

In the case that an annotated sequence contains an instance B of one family inserted into the middle of an instance A of another family, the above DP mechanism will annotate the sequence in a form A_1BA_2. PolyA takes steps to identify the relationship between A_1 and A_2 as ordered fragments of A (see Figure 2.2). To achieve this, a graph is created in which each labeled sequence block is represented as a vertex, and a directed edge is established between the vertices corresponding to adjacent segments. Additional edges are added to the graph for each pair of vertices corresponding to segments might share to the same family, specifically: (i) the alignments supporting the two segments are relatively co-linear in the label's consensus sequence, and (ii) the label with highest confidence on one of the segments has some non-negligible (default $\geq 1\%$) confidence on the other segment (tested in both directions). In such a graph, an inserted element will appear as a vertex with in-degree and out-degree of 1. PolyA removes all such vertices from the graph, splices the corresponding positions from the confidence-based DP matrix, and repeats the DP trace. With the inserted sequence removed, the adjusted transition opportunities enable stitching of previously-separated segments. This process is iterated until no inserted sequences remain.

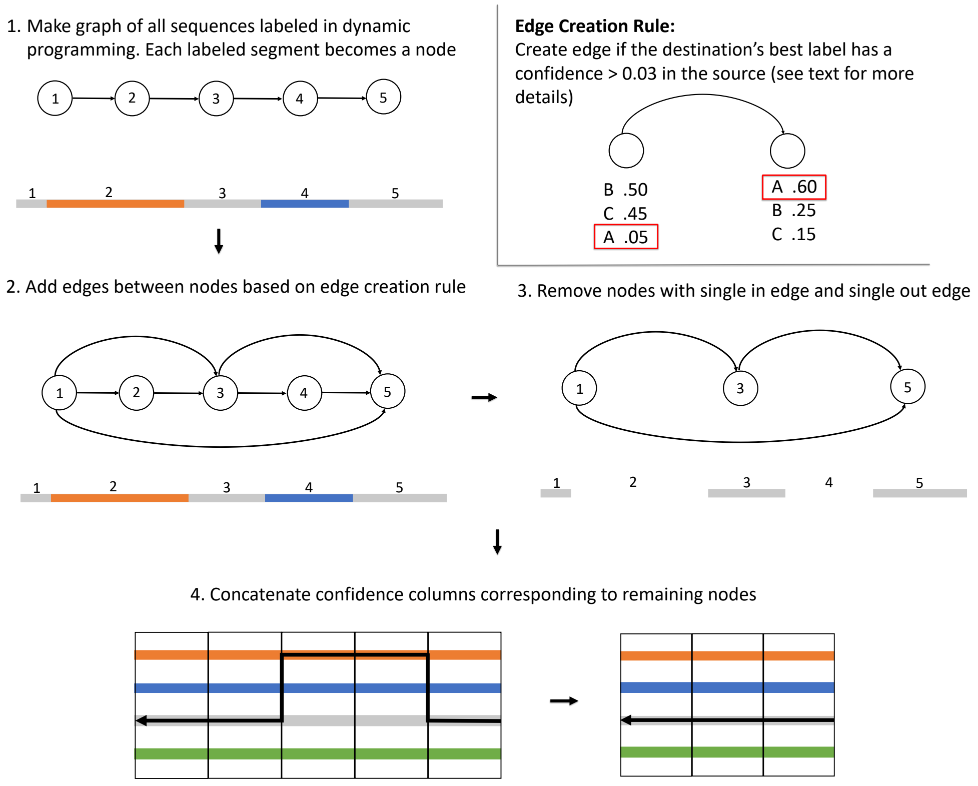
1. Make graph of all sequences labeled in dynamic programming. Each labeled segment becomes a node
1
2
3
4
5
Edge Creation Rule:
Create edge if the destination's best label has a confidence > 0.03 in the source (see text for more details)
B .50
C .45
A .05
A .60
B .25
C .15
2. Add edges between nodes based on edge creation rule
3. Remove nodes with single in edge and single out edge
4. Concatenate confidence columns corresponding to remaining nodes

Figure 2.2: Graph algorithm steps for identifying inserted elements, splicing them out, and stitching segments of the sequence that has been inserted into back together as the original element.

CHAPTER 3 RESULTS

Results

To annotate with PolyA, the target (to-be-annotated) sequence should be aligned to all the sequences in the annotation database. Alignment may be performed with any sequence-to-sequence alignment tool that depends on a scoring matrix (e.g. blast [10] or cross_match [11]). For the results presented here, this alignment is performed with cross_match, since this is the most sensitive alignment method used in RepeatMasker for consensus sequences; the annotation database is the Repbase RepeatMasker Edition library (a future version of PolyA will accept alignments with profile hidden Markov model databases such as Dfam and Pfam; see Discussion). PolyA takes as input (i) the collection of alignments between the target sequences and the database, and (ii) a reference to the scoring matrix and gap parameters used to produce each alignment. As described above, PolyA computes a measure of the confidence with which each position of the target can be assigned to each competing annotation candidate. These position-specific confidence estimates for all competing annotations support identification of transition points generated by forces such as recombination and transposable element integration, and enable boundary detection between adjacent elements with overlapping competing annotations. The dynamic programming approach described above identifies a highest-confidence path through competing annotations, assigning labels to each position of the target sequence. This is followed by a stage that iteratively identifies insertion events and stitches the segments that were split by such insertions. The result is an annotation adjudication that correctly addresses events that typically cause incorrect labeling, and also discloses a measure of annotation certainty.

To evaluate the efficacy of PolyA, we constructed a variety of artificial sequences with known origin, insertion activity, and recombination breakpoints. In each case, artificial sequences were constructed by mutating consensus sequences from Repbase, according to average substitution, insertion, and deletion rates acquired from the RepeatMasker hg38.fa.out annotation file [4], then inserting, trimming, and recombining as appropriate for the specific scenario being assessed.

Annotation Confidence

In [5] we introduced a simple mechanism for computing annotation confidence when several competing candidates produce alignments to a sequence window (see Methods). This confidence measure decreases as mutational load of an annotated sequence increases. To demonstrate this, we selected the AluY subfamily consensus sequence, and for each integer value in the range $p \in [1..50]$, generated 100 mutated copies of AluY in which p percent of nucleotides were randomly selected, and modified (uniformly) to a different nucleotide. Each mutated instance was aligned to all Repbase Alu subfamily consensus sequences using cross_match, and Eq 2.2 was applied to compute the confidence with which the instance was assigned an annotation of AluY. Figure 3.1 provides the average confidence for each bin of 100 (dark line), along with a shaded region indicating an interval of 1 standard deviation. This plot provides a sense of the decay in confidence expected as sequence divergence increases; specific confidence details for a particular (sub)family will depend on the number and relationship of similar subfamilies.

Selecting Change-point for Overlapping Annotation Candidates

When faced with competing, overlapping annotation candidates, PolyA infers a precise intermediate boundary between overlapping annotation candidates by computing per-residue confidence values and identifying a highest-confidence trace. This approach is effective for recombinations and insertions as described below, as well as for overlapping neighbors as demonstrated in Fig 3.2, in which the tail of an L1M1_orf2 candidate overlaps with several competing Alu alignments. The bottom of Fig 3.2 represents the position-specific confidence values as a heatmap, with green representing high confidence and purple representing low confidence (Note: the Alu shows long stretches

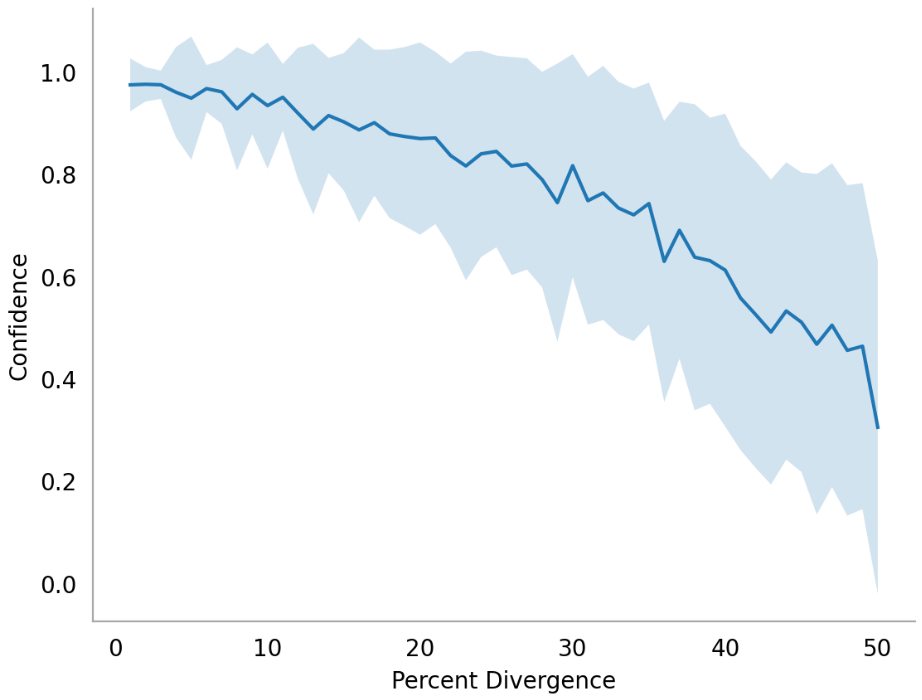

Figure 3.1: **Confidence as a function of sequence divergence.** Beginning with the Repbase consensus sequence for the AluJr subfamily, mutated instances were created with a range of percent substitutions, with 100 copies for each percentage bin. Each mutated instance was aligned to all Alu subfamilies using cross_match (25p41g matrix, gap_init=-25, and gap_ext=-5). For each sequence, the confidence in AluJr as the correct annotation was captured. The dark blue line shows the average AluJr confidence per bin, and the shaded region shows the range of a single standard deviation.

of low confidence because that region of the genome is equally-well explained by several other Alu subfamilies - all of them share equally-low confidence over that region).

Recombination

The presence of many highly-similar TE instances in a genome leads to common occurrence of non-allelic homologous recombination [12, 13], in which the initial sequence a is replaced in part by a subsequence of some homolog b. If a and b belong to different subfamilies A and B, respectively, then the sequence alignment step of annotation is likely to find near-full-length alignments of the sequence to database representatives of both A and B; the alignment to the A representative will

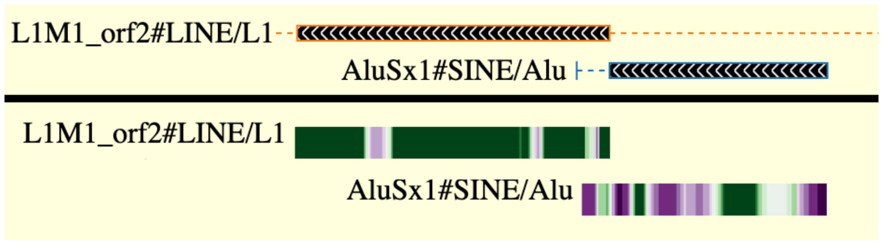

Figure 3.2: **Detecting the change-point between overlapping elements; demonstration of confidence heatmap.** This region of the human genome (hg38, chr10:58800-59500) contains a fragment of an L1M1 element, overlapping the tail of an AluSx1 candidate annotation. The heatmap on the bottom represents the residue-specific confidence computed in PolyA, with dark green = high confidence, dark purple = low confidence, and moderate confidence represented by lighter colors and white. To limit visual clutter, this heatmap shows only the confidence heatmaps for the two 'winning' annotations; others are hidden from view. The top half of the figure shows the final PolyA adjudication, in which the region in which the competing annotations overlap is assigned to the higher-confidence L1M1 annotation.

be relatively poor in the region that was replaced by a stretch of sequence b, and vice versa. Using the standard adjudication process, the alignment with the higher score will be selected, and the existence of recombination will not be annotated.

PolyA computes residue-specific annotation confidence estimates, and uses them to infer the presence, location, and identity of such recombinations. Figure 3.3 shows an example of an apparent recombination that is missed by the standard best-score-wins approach, but is detected by PolyA.

Identification of homologous recombination is sure to be imperfect: (1) recombination events with highly similar donor and acceptor sequences, or with short donor segments, are relatively unlikely to be recognized, and (2) non-recombined sequence elements that are highly diverged from their appropriate consensus sequence are at increased risk of recombination false positive (due to reduced confidence as in Figure 3.1). We aimed to quantify sensitivity and false annotation by generating a large number of simulated sequences. In the following sections we describe the creation of these simulated benchmarks, and accompanying assessment. For all benchmarks based on simulated sequences, alignments were performed using cross_match, with fixed parameters consisting of the 25p41g matrix (available at https://github.com/Dfam-consortium/RepeatModeler), gap_init=-25, and gap_ext=-5.

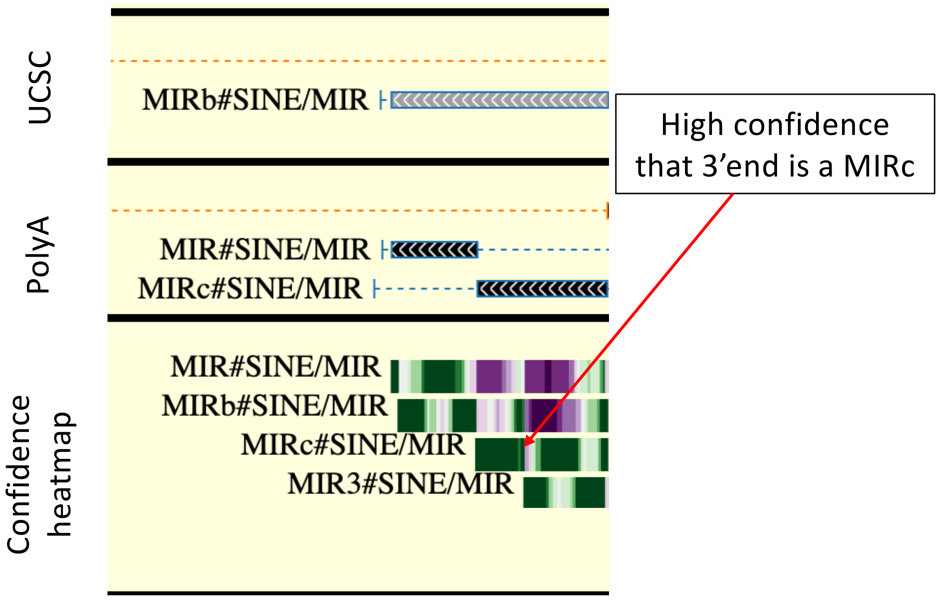

Figure 3.3: **Recombination example.** The top panel shows the repeatmasker-adjudicated annotation of human (hg38) chr19:15304678-15304839 as a full-length MIRb element. The bottom panel presents a heatmap of the windowed average confidence that serves as the basis of PolyA adjudication, which highlights that in the 3' end of the region, MIRc is the prefered annotation with high confidence. The middle panel shows that PolyA recognizes a recombination between MIR and MIRc at roughly the midpoint of the extant sequence window. The standard repeatmasker preference for MIRb is due to the fact that it has the largest score of all candidates (MIRb=349, MIR=280, MIRc=290, MIR3=196). In the 3' half of the annotated region beginning at position 15304742, MIRb's score is 269, while MIRc's score is 290.

False Positive Recombination

We first sought to test the frequency with which PolyA incorrectly identifies a sequence as being the result of a recombination, specifically: how often does PolyA claim that a sequence element is derived from two subfamilies, even though the actual sequence is derived from a single subfamily. We began with Alu sequences: randomly selecting one Alu type (AluS, AluJ, AluY), then one subfamily within the selected type, among those found in Repbase. The consensus sequence corresponding to the selected subfamily was mutated with subfamily-specific rates of substitution, insertion, and deletion. Substitution rates were approximated from existing repeatmasker (RM) annotations, modeling transitions as twice as likely as transversions. Indel rates and lengths were also chosen based on RM annotations: an overall length distribution of insertions and deletions (capped at length 7) was computed from all RM alignments, and used as the basis for randomly selecting indel

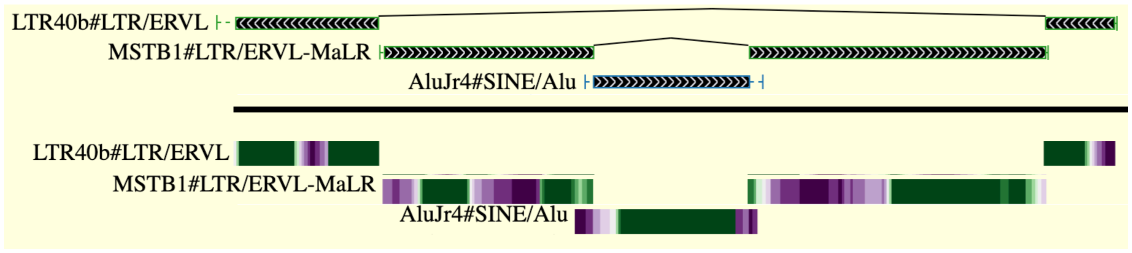

Figure 3.4: **Example of nested insertions.** This region of the human genome (hg38, chr11:11990878..11991874) exemplifies nested transposable element insertions. Here, an instance of AluJr was inserted within an instance of MSTB1, which itself was inserted into an instance of LTR40b. The confidence heatmap is included for reference, and demonstrates a change-point decision in the context of nested annotations; heatmaps for competing annotations are not shown, in order to reduce visual clutter. PolyA automates the splicing of inserted elements and stitching of the surrounding split segments.

lengths; for each benchmark instance, such indels were accumulated until reaching family-specific indel averages determined from RM annotations. This was repeated 10,000 times, yielding 10,000 sequences that contain no recombination and should be identified as such. These sequences were aligned to all Alu subfamily consensus sequences using cross_match, and adjudicated using PolyA. Of these Alu sequences, 99.8% were correctly identified as being derived from a single subfamily. The same procedure was performed to produce 10,000 L1 instances, randomly selecting among all Repbase L1 subfamilies. Of these, 97.8% were correctly identified as having a single source.

True Positive Recombination

To assess PolyA's sensitivity in detecting the aftermath of recombination, we performed experiments similar to those above, but now *with* recombination. Beginning with Alu, we: (i) selected a pair of distinct Alu subfamily consensus sequences a and b, with uniform probability as described above, (ii) aligned a and b using cross_match, and (iii) identified the middle position i of the alignment. If in the resulting sequence halves, either was shorter than 50 nucleotides, the simulation for this pair was aborted. With surviving simulations, (iv) both a and b were mutated as above, then (v) a recombinant sequence was created, made up of the prefix of a up to the nucleotide corresponding to position i of the alignment and the suffix of b beginning just after the ith position. This was repeated until 10,000 sequences were successfully generated, producing 10,000 simulated recombined sequences. We call these simulated sequences, with one end from a and one end from b, 'single-recombinations'. Each resulting sequence was aligned to all Repbase Alu consensus sequences with cross_match, residue-specific confidence estimates were computed, and these were used to label the entire sequence allowing for recombination.

From these simulated Alu single recombinants 55.1% were correctly identified as recombinants. Among these, 65.2% were assigned to the correct subfamily on both ends of the recombination, while 96.9% were correctly assigned on at least one half.

A similar procedure was followed to produce L1 single-recombinations. Because Repbase L1 sequences are fragments of a full L1 (corresponding to 3' end, 5' end, and internal ORF region), many pairs do not meaningfully overlap. Furthermore, highly-divergent sequences are unlikely to produce homologous recombination. We performed an all-vs-all alignment of Repbase L1 consensus sequences, and identified 1553 alignment regions with length $\geq$ 100 bp on both sequences and $\geq$ 90% identity. With a given sequence-pair, we selected a random breakpoint and produced a recombinant as above, repeating 7 times for each pair, yielding a total of 10,871 L1 single-recombinations. These were each aligned using cross_match to the full contingent of Repbase L1 consensus sequences, with resulting alignments input to PolyA. Because PolyA adjudicates between annotation candidates produced by the alignment tool, it will fail to assign a correct family to a region if the input from the precursor alignment software does not include the correct family. This occurred in 5 L1 inputs. These have no possibility of being correctly adjudicated and were removed from the analysis. Of the remaining inputs, 94.8% of simulated L1 recombinants were correctly identified as recombinants. Among these, 93.6% were assigned to the correct subfamily on both ends of the recombination, while 99.8% were correctly assigned on at least one half.

True Positive Gene Conversions

We repeated the above experiment for sequences simulating gene conversion, in which an internal segment of the original sequence is replaced by sequence from a related subfamily. Specifically, we identified two subfamilies and aligned their consensus sequences a and b as before, then *two* recombination points i and j were identified at positions 1/3 and 2/3 into the alignment, aborting construction of sequences where all segments are not atleast 50 nucleotides in length. For the remaining simulations both sequences were mutated, and the segment from sequence a corresponding to alignment positions i through j was replaced with the corresponding segment from sequence b. As before, 10,000 simulated sequences were produced from the Alu family, and for the L1 family 1228 alignment regions $\geq 90\%$ identity and that fulfill the length requirement were identified. Repeating the gene conversion sequence construction described above 9 times for each pair we produced 11052 sequences. For these 'internal recombinations', 4 L1s were thrown out because input alignments from cross_match did not include the correct subfamily alignments. Among surviving instances, only 2.7% of simulated Alus were correctly identified as containing an internal recombination, while 18.1% were correctly identified as resulting from *some* recombination (i.e. were annotated as a single-recombinant). For L1 simulations, 56.5% were correctly identified as being the result of internal recombination, while 63.3% were correctly identified is being the result of *some* recombination(s) (i.e. at least one part of the recombination was recognized).

In both experiments, the low recombination sensitivity in Alus is not particularly surprising, since the nucleotides typically used to discriminate one of the subfamilies may not even have made it into the final recombinant sequence. Particularly for internal recombinations, the component sequences are all typically short enough that discriminating nucleotides are likely to be missing, leading to annotation ambiguity.

Stitching Annotations Fragmented by Nested Insertions

It is common to find a single instance of a younger TE (sub)family inserted inside an instance of an older TE (sub)family. A goal of PolyA is to support the automatic stitching of the segments separated by such (possibly-nested) insertions. This is achieved by repeatedly identifying an inserted element, splicing it from between the sequence fragments that it separated, then repeating the labeling process on the resulting stitched sequences. This procedure is repeated until no apparent insertions are observed (see Methods for details). Figure 3.4 shows a genomic region with nested inserted elements. PolyA first identified a series of confidently-annotated segments, then spliced the inner-most element (AluJr4), stitching the remaining sequence around the excision. The resulting full-length MSTA1 was then spliced, so that the surrounding LTR40a instance could be stitched, and identified in full.

To assess the efficacy of PolyA's annotation stitching mechanism, we simulated 3 classes of nested architectures, which we represent here as short strings: ABA (a single fragment of family B inserted into an instance of family A), $ABACA$ (distinct fragments from families B and C,each inserted into an different location in an instance of family A), and $ABCBA$ (a nested insertion, in which a fragment of family C is inserted into a fragment of family B, which itself is inserted into an instance of family A).

ABA sequences were simulated by creating 1,000 each of Alu1-Alu2-Alu1 (with Alu2 being a younger subfamily than Alu1), MER-Alu-MER, and MIR-MER-MIR amalgams. These are not meant to be exhaustive, but are representative of the kinds of insertions seen in the human genome. Alu families were selected as above, and others were selected randomly. In each case, the inner sequence was trimmed to retain the middle 2/3 of its length, and inserted into the middle of the outer sequence, splitting the outer sequence, but not replacing it. Trimming of the inner sequence was performed in order to replicate the common situation in TE annotation in which the boundary between inserted and surrounding sequence is unclear; this is a decidedly artificial arrangement, but it replicates the challenge faced during adjudication. Each of these 3,000 were aligned against the entire Repbase database, with results fed to PolyA. Of these, 182 sequences were filtered because the correct families were not among the cross_match results.

$ABACA$ sequences were simulated by creating 1,000 each of LTR-L1^1-LTR-L1^2-LTR (in which L1^1 and L1^2 are two distinct L1 subfamilies), HAL1-Alu^1-HAL1-Alu^2-HAL1 (with distinct subfamilies Alu^1 and Alu^2), and L2-MER^1-L2-MER^2-L2 (with distinct subfamilies MER^1 and MER^2). In all other ways, these are produced as with the ABA format. Of these, 172 were filtered because the correct families were not among the cross_match results.

$ABCBA$ sequences were simulated by creating 1,000 each of HAL1-MER-Alu-MER-HAL1, L4-

MST-Alu-MST-L4, and L2-LTR-MST-LTR-L2. Of these, 122 were filtered due to failed cross_match results.

Table 3.1 shows that the correct nesting architecture was usually identified, as were the correct subfamilies.

Table 3.1: Accuracy results when annotating nested sequences.

	correct nesting architecture	correct families
ABA	93.3%	83.4%
$ABACA$	77.8%	92.4%
$ABCBA$	68.1%	92.2%

Accurate Boundary Locations

To evaluate the accuracy of boundary point detection in PolyA, we computed the distance between estimated and true boundaries for all artificial sequences described in the experiments above (distance = |actual - detected|). The mean and median boundary detection error produced by PolyA is 5 and 9 nucleotides, respectively. Figure 3.5 shows the distribution of boundary detection error. Precise accuracy statistics depend on specifics of benchmark creation, alignment software choice, and aligner parameterization, but these results suggest that PolyA is effective at identifying cross-point boundaries.

Short tandem repeats

When annotating genomic sequences, it is common to mask short tandem repeats (STRs) prior to alignment-based annotation, either *hard-masking* (changing a masked region to a sequence of Ns so that alignment software assigns no score to alignments to the masked region) or *soft-masking* (marking a region such that that it will not serve as the seed of an alignment, but can be used in scoring after seeding is complete). PolyA accepts scored STR annotations from ULTRA [9] among candidate annotations. The left side of Fig 3.6 demonstrates how this may effectively

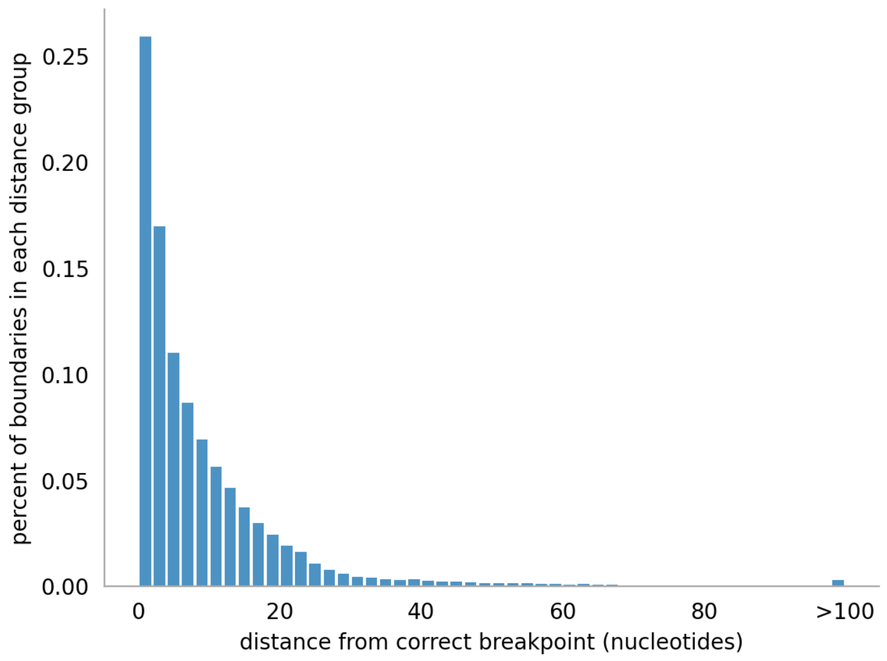

Figure 3.5: **Boundary accuracy.** To evaluate the accuracy of boundary point detection in PolyA, we computed the distance between estimated and true boundaries for all artificial sequences described above. All 24,961 simulated sequences that were correctly-labeled as recombinations or nestings were used. The boundary error for each annotation was assigned to a bin of size 2. In 90% of all such annotations, the predicted boundary was within 20 nucleotides of the true boundary.

allow an STR to out-compete a potential fragmentary family annotation (replacing a weak L1MC4 fragment annotation seen on UCSC based on repeatmasker's default adjudication) with the more appropriate STR call. The right side of Fig 3.6 shows an example of an STR candidate that is out-competed by the A-rich 3' tail of an AluSz annotation.

In practice, it is likely still useful to soft-mask a genome prior to annotation, in order to limit excessive run time caused by evaluating alignments seeded in STR regions. Even so, by enabling direct competition between annotations from a library (by sequence alignment) or of STRs (as by ULTRA), PolyA provides substantially better fine-grained resolution of annotation near repetitive regions.

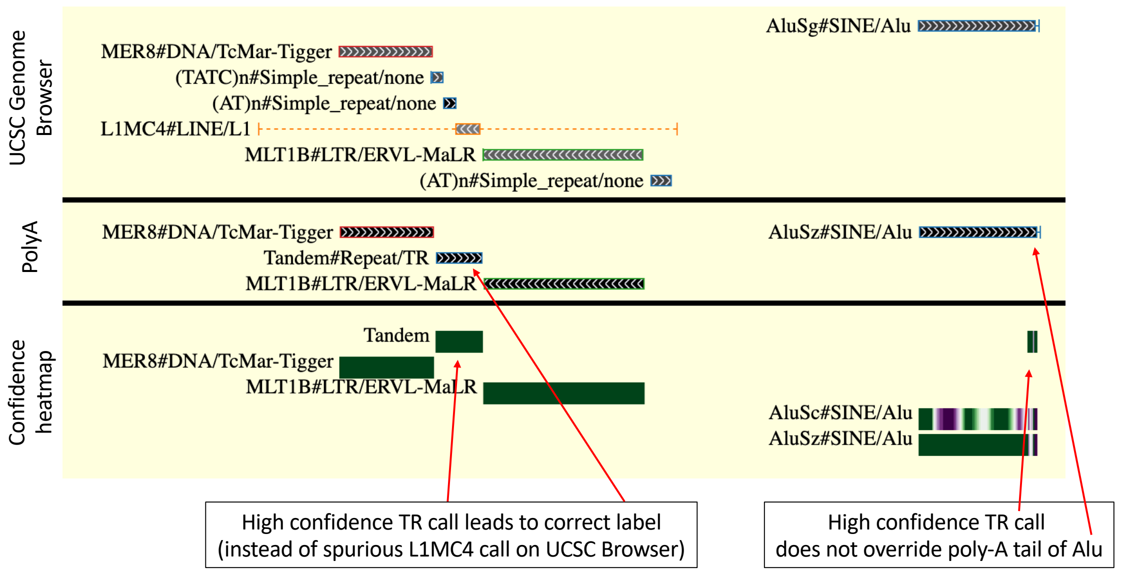

Figure 3.6: **Adjudicating short tandem repeats.** The top section shows the annotation of hg38, chr1:14632106..146333918 as presented on the UCSC genome browser, which is derived from the standard adjudication results in repeatmasker, using ProcessRepeats. This process aligns the library against genomic sequence that has first been masked for tandem repeats using TRF; it reports a short L1MC4 fragment of dubious accuracy (left), and a reasonable full-length AluSg annotation (right). The middle section shows the annotation produced when candidate annotations from repeatmasker (TEs) and ULTRA (tandem repeats) are adjudicated using PolyA; it identifies the dubious L1MC4 fragment instead as a tandem repeat (left), and agrees on the Alu designation on the right (though subtle confidence differences lead to an AluSz assignment). The bottom section presents a confidence heatmap over the region. Of particular interest is the poly-A region on the far right of the plot; ULTRA correctly identifies this region as repetitive, but continuity with the preceding Alu annotation causes the region to be correctly labeled as part of the Alu.

CHAPTER 4 DISCUSSION

PolyA produces annotation confidence estimates for biological sequences based on an input of candidate sequence alignments and underlying scoring matrices. These confidence estimates are computed on a per-residue basis, and used to infer transitions between overlapping annotations, including those caused by recombination and (possibly-nested) insertion of one element into another. We have demonstrated the efficacy of PolyA on multiple simulated scenarios, and shown that it produces reasonable results on the human genome. We are currently working to incorporate PolyA into the RepeatMasker software package for transposable element annotation.

PolyA often fails to identify recombination among instances of highly similar Alu elements - this is not surprising because (i) genomic Alu fragments are often short (e.g. less than 50 nucleotides), and thus unable to accumulate enough support to overcome transition penalties, and (ii) Alu subfamily sequences are highly similar, often differing by only a few nucleotides. We view this as a feature, not a failure. Importantly, PolyA produces confidence values for all annotations, and is therefore able to communicate the diminished confidence resulting from alignments to multiple highly-similar sequence elements, as with highly similar Alu subfamilies. We expect both the annotation tracing and confidence measures to contribute to future improvements in genome browser presentation of annotations.

In the current release, PolyA adjudicates annotations based on only nucleotide sequence-to-sequence alignments using scoring matrices, supplemented with tandem repeat annotations from ULTRA [9]. In a future release, PolyA will accept (i) annotations of protein sequences, and (ii) alignments made with profile hidden Markov models, which are the basis of sequence-family databases such as Dfam [1] and Pfam [2].

In its current form, PolyA naively adjudicates between candidate annotations without regard for additional information that expert systems currently use to improve annotation quality. In the future, we will explore approaches such as (i) adjusting transition penalties to prefer full length insertions when supported (akin to preferring global alignment [14]), and (ii) adjusting transition penalties based on relative apparent divergence of a sequence window to its candidate annotation.

BIBLIOGRAPHY

[1] R. Hubley, R. D. Finn, J. Clements, S. R. Eddy, T. A. Jones, W. Bao, A. F. Smit, and T. J. Wheeler, "The dfam database of repetitive dna families," *Nucleic acids research*, vol. 44, no. D1, pp. D81–D89, 2016.

[2] S. El-Gebali, J. Mistry, A. Bateman, S. R. Eddy, A. Luciani, S. C. Potter, M. Qureshi, L. J. Richardson, G. A. Salazar, A. Smart *et al.*, "The pfam protein families database in 2019," *Nucleic acids research*, vol. 47, no. D1, pp. D427–D432, 2019.

[3] E. P. Nawrocki, S. W. Burge, A. Bateman, J. Daub, R. Y. Eberhardt, S. R. Eddy, E. W. Floden, P. P. Gardner, T. A. Jones, J. Tate *et al.*, "Rfam 12.0: updates to the rna families database," *Nucleic acids research*, vol. 43, no. D1, pp. D130–D137, 2015.

[4] Smit, AFA. Hubley, R., Green, P., "Repeatmasker open-4.0.2013-2015," 2013. [Online]. Available: http://www.repeatmasker.org/

[5] K. Carey, G. Patterson, and T. Wheeler, "Transposable element subfamily annotation is unreliable," *Mobile DNA (in review, preprint)*, 2020.

[6] Y.-K. Yu and S. F. Altschul, "The construction of amino acid substitution matrices for the comparison of proteins with non-standard compositions," *Bioinformatics*, vol. 21, no. 7, pp. 902–911, 2005.

[7] M. C. Frith, "How sequence alignment scores correspond to probability models," *Bioinformatics*, vol. 36, no. 2, pp. 408–415, 2020.

[8] A.-K. Schultz, M. Zhang, T. Leitner, C. Kuiken, B. Korber, B. Morgenstern, and M. Stanke, "A jumping profile hidden markov model and applications to recombination sites in HIV and HCV genomes," *BMC bioinformatics*, vol. 7, no. 1, p. 265, 2006.

[9] D. Olson and T. Wheeler, "Ultra: A model based tool to detect tandem repeats," in *Proceedings of the 2018 ACM International Conference on Bioinformatics, Computational Biology, and Health Informatics*, 2018, pp. 37–46.

[10] S. F. Altschul, W. Gish, W. Miller, E. W. Myers, and D. J. Lipman, "Basic local alignment search tool," *Journal of molecular biology*, vol. 215, no. 3, pp. 403–410, 1990.

[11] Green, P., "Phrap and cross_match." [Online]. Available: http://www.phrap.org/phredphrap/phrap.html

[12] J. A. Fawcett and H. Innan, "The role of gene conversion between transposable elements in rewiring regulatory networks," *Genome biology and evolution*, vol. 11, no. 7, pp. 1723–1729, 2019.

[13] P. Sung and H. Klein, "Mechanism of homologous recombination: mediators and helicases take on regulatory functions," *Nature reviews Molecular cell biology*, vol. 7, no. 10, pp. 739–750, 2006.

[14] M. Brudno, S. Malde, A. Poliakov, C. B. Do, O. Couronne, I. Dubchak, and S. Batzoglou, "Glocal alignment: finding rearrangements during alignment," *Bioinformatics*, vol. 19, no. suppl_1, pp. i54–i62, 2003.

[15] W. Bao, K. K. Kojima, and O. Kohany, "Repbase update, a database of repetitive elements in eukaryotic genomes," *Mobile Dna*, vol. 6, no. 1, p. 11, 2015.

[16] A. Harpak, X. Lan, Z. Gao, and J. K. Pritchard, "Frequent nonallelic gene conversion on the human lineage and its effect on the divergence of gene duplicates," *Proceedings of the National Academy of Sciences*, vol. 114, no. 48, pp. 12 779–12 784, 2017.